

## Frequency evaluation of MIKES AHM3 by MIKES-Sr+1 for the period MJD 61059 to 61064

The frequency of the hydrogen maser (HM) MIKES AHM3 (1404189) was evaluated during the 5-day period MJD 61059 to 61064 using the  $^{88}\text{Sr}^+$  optical single-ion frequency standard MIKES-Sr+1 (1784101) and an optical frequency comb. The  $^{88}\text{Sr}^+$  standard operated for 94.1% of the period. The evaluation is based on the 2025 recommended frequency for the  $5s\ ^2S_{1/2} \rightarrow 4d\ ^2D_{5/2}$  transition in  $^{88}\text{Sr}^+$ , 444 779 044 095 485.347 Hz, with a fractional uncertainty of  $1.7 \times 10^{-16}$  [1]. The results of the evaluation are given in Table 1. The operation and uncertainty evaluation of MIKES-Sr+1 are described in [2] and summarized below.

Table 1: Results of the evaluation of AHM3 by MIKES-Sr+1.

Period of estimation	$y(\text{AHM3}/\text{Sr+1})$ / $10^{-15}$	$u_A$ / $10^{-15}$	$u_B$ / $10^{-15}$	$u_{A/\text{Lab}}$ / $10^{-15}$	$u_{B/\text{Lab}}$ / $10^{-15}$	$u_{\text{Srep}}$ / $10^{-15}$	Uptime %
61059–61064	639.65	0.0033	0.0028	0.11	0.020	0.17	94.1

### 1 Measurement configuration

The measurement configuration is schematically shown in Fig. 1. The clock laser is a 1348 nm external-cavity diode laser (ECDL). In contrast to the work in [2], it is now stabilized to an 18 cm vertical ultra-low-expansion (ULE) glass cavity. The light to the ion is frequency doubled to 674 nm. The light to the ion and the frequency comb is de-drifted by an acousto-optic modulator (AOM, frequency  $f_{\text{drift}}$ ) based on feedback from the ion. Using another AOM (frequency  $f_{\text{Zeeman}}$ ), independent servo loops track six Zeeman components of the clock transition, whose mean is free from linear Zeeman shift and tensor shifts. The fibre frequency comb is optically locked to the clock laser. The frequency ratio between the HM and MIKES-Sr+1 is determined from the

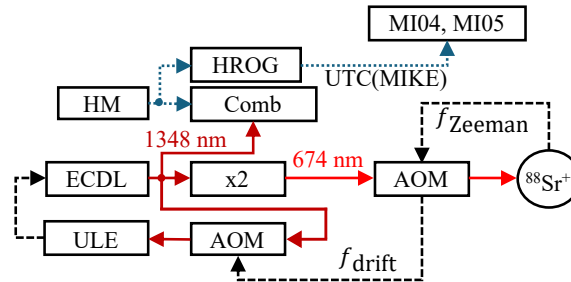


Figure 1: Clock-laser setup and frequency chain to the  $^{88}\text{Sr}^+$  ion, frequency comb, hydrogen maser (HM), and geodetic GNSS receivers MI04 and MI05 for time transfer. HROG—high resolution offset generator. Solid (dotted) lines indicate optical (rf) signals, while dashed lines indicate feedback loops for Pound-Drever-Hall locking (left), drift compensation of the cavity ( $f_{\text{drift}}$ , middle), and tracking the Zeeman components of the clock transition ( $f_{\text{Zeeman}}$ , right). AOMs for fiber noise cancellation are not shown.

AOM frequencies, the in-loop beat note between the clock laser and the comb, and from the comb repetition rate and carrier offset frequency measured against the HM. For details, see [2].

## 2 MIKES-Sr+1 evaluation

A detailed uncertainty evaluation is presented in [2]. The statistical uncertainty  $u_{A,i}$  of a particular measurement  $i$  is estimated from a  $\tau^{-1/2}$  fit to the clock self-comparison instability evaluated at the total measurement time  $\tau_i$  (including valid data only). The instability varies with the probe time (and dead time). During this evaluation period, it was on average  $2.1 \times 10^{-15} \tau^{-1/2}$ . The total  $u_A$  of the period is determined as  $u_A = (\sum_i w_i^2 u_{A,i}^2)^{1/2}$ , where the weights are proportional to the duration of the individual measurements,  $w_i = \tau_i / (\sum_i \tau_i)$ .

Several systematic frequency shifts are evaluated dynamically. Several systematic uncertainty contributions  $j$  also depend on parameters such as the probe time (light shifts, thermal motion shifts via the ion heating rate), the Zeeman AOM rf power (AOM chirp), the trap drive voltage (blackbody radiation shift), and the electric quadrupole shift and excess micromotion measured during a clock run. Each uncertainty contribution is assumed to be fully correlated throughout the evaluation period so that its weighted mean is  $u_{B,j} = \sum_i w_i u_{B,i,j}$ . The total systematic uncertainty is then evaluated as  $u_B = (\sum_j u_{B,j}^2)^{1/2}$ . An uncertainty budget for the evaluation period is shown in Table 2.

Due to the Fennoscandian land uplift (postglacial rebound), the height of the clock relative to the reference potential  $W_0 = 62\,636\,856.00 \text{ m}^2/\text{s}^2$  increases by 3.8 mm/y. For simplicity, this evaluation has been automated based on the mean epoch of a particular measurement. The uncertainty of the gravitational redshift,  $2.4 \times 10^{-18}$ , is added in quadrature to that of the clock itself. Tidal effects are neglected due to our high uptime and because the amplitude of solid Earth tides decreases with increasing latitude [3] (MIKES's latitude is 60.2°).

## 3 Frequency comparison

The measured maser frequency and the uptime of MIKES-Sr+1 for the evaluation period are shown in Fig. 2. The statistical uncertainty  $u_{A/\text{Lab}}$  includes the uncertainty due to the dead time of MIKES-Sr+1 (DTU). The DTU consists of a deterministic part due to the HM drift and a stochastic part. The frequency in the middle of the evaluation period is obtained by correcting the measured mean frequency using the drift and the offset between the middle point and the barycenter of the data. The drift was estimated from a linear fit over the evaluation period. The noise model for the maser is given in Table 3. As in [5], the bump in the power spectral density, caused by quasi-periodic frequency jumps, is described by a Lorentzian peak. The extrapolation uncertainty is evaluated using the Fourier transform method [6].

The UTC( $k$ )-HM data is submitted to the BIPM with a resolution of 0.1 ns. The standard deviation of the rectangular distribution of rounding errors is  $u_{x,\text{round}} = 0.1/\sqrt{12}$  ns. When evaluating the mean frequency over a period of duration  $T$ , this gives rise to a fractional uncertainty  $u_{y,\text{round}} = \sqrt{2}u_{x,\text{round}}/T \approx 4.7 \times 10^{-16}/(T/\text{d})$ . The statistical uncertainty of the measurement itself is estimated to be  $u_{y,\text{meas}} \approx 2.7 \times 10^{-16}/(T/\text{d})$ , including the 1 PPS signal distribution. The total UTC( $k$ )-HM uncertainty is included in  $u_{A/\text{Lab}}$ .

An upper limit of  $2 \times 10^{-17}$  for the systematic uncertainty  $u_{B/\text{Lab}}$  was estimated in a comparison between two frequency combs with independent rf distribution [2]. The corresponding statistical uncertainty was found to be negligible compared to  $u_{B/\text{Lab}}$  for relevant measurement times and is not included in  $u_{A/\text{Lab}}$ . The  $u_{A/\text{Lab}}$  and  $u_{B/\text{Lab}}$  contributions are summarized in Table 4.

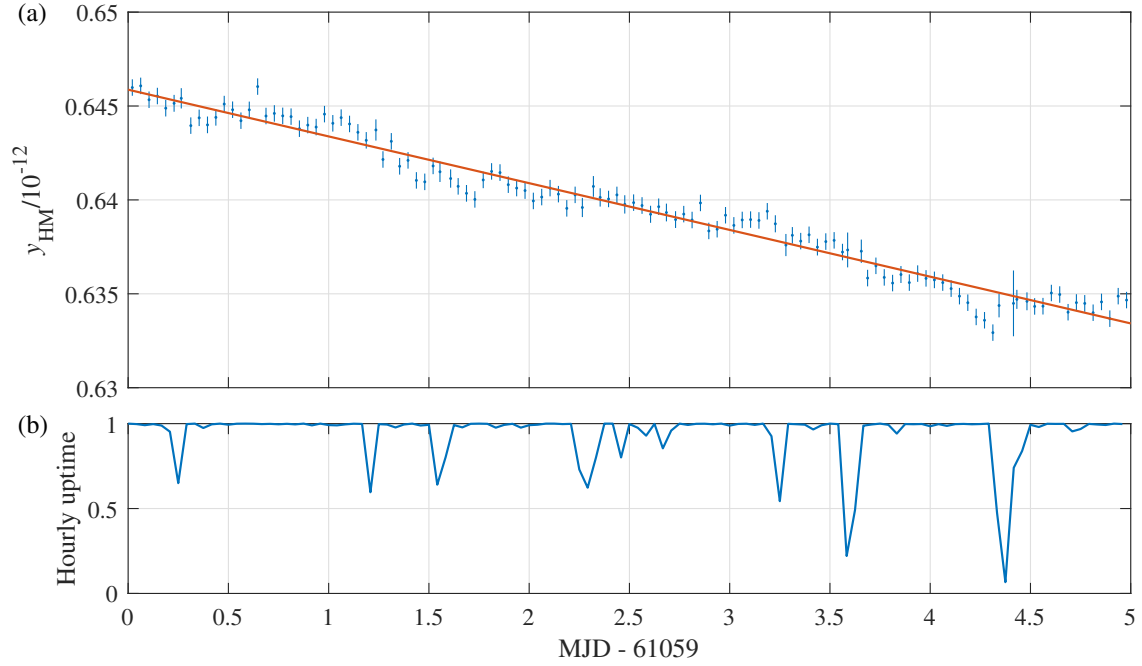


Figure 2: (a) Maser fractional frequency as measured against MIKES-Sr+1 in 1 h wall-clock bins (dots). The error bars are the Allan deviation at an integration time corresponding to the number of valid 1 S/s points in the bin and the line is a linear fit. (b) Hourly uptime of MIKES-Sr+1 over the evaluation period (total uptime 94.1%).

## References

- [1] BIPM, [Recommended values of standard frequencies](#).
- [2] T. Lindvall *et al.*,  $^{88}\text{Sr}^+$  optical clock with  $7.9 \times 10^{-19}$  systematic uncertainty and its absolute frequency with  $9.8 \times 10^{-17}$  uncertainty, [Phys. Rev. Applied](#) **24**, 044082 (2025).
- [3] C. Voigt *et al.*, Time-variable gravity potential components for optical clock comparisons and the definition of international time scales, [Metrologia](#) **63**, 1365 (2016).
- [4] T. Lindvall *et al.*, Measurement of the Differential Static Scalar Polarizability of the  $^{88}\text{Sr}^+$  Clock Transition, [Phys. Rev. Lett.](#) **135**, 043402 (2025).
- [5] T. Lindvall *et al.*, Coordinated international comparisons between optical clocks connected via fiber and satellite links, [Optica](#) **12**, 843–852 (2025).
- [6] S. T. Dawkins *et al.*, Considerations on the measurement of the stability of oscillators with frequency counters, [IEEE Trans. Ultrason., Ferroelectr., Freq. Control](#) **54**, 918 (2007).

Table 2: Uncertainty budget for MIKES-Sr+1 for the reported evaluation period ( $10^{-18}$ ).

Contribution	Shift	Uncertainty
Blackbody radiation (BBR) E1 shift	524.69	
BBR field		0.28
Differential polarizability $\Delta\alpha_0^\dagger$		0.22
Dynamic correction $\eta$		0.090
BBR M1 shift	-0.0102	0.0002
Collisional shift	0.00	0.22
Thermal motion shifts	-2.6	1.1
Electrical quadrupole shift	0.000	0.043
Excess micromotion shifts	0.0000	0.0003
Tensor Stark shift	0.000 00	0.000 09
1092 nm ac Stark shift	0.00	0.12
674 nm E1 ac Stark shift	0.004	0.006
674 nm E2 ac Stark shift	0.000	0.003
Quadratic Zeeman shift, static field	0.200	0.004
AOM chirp	0.00	0.13
Servo errors	0.00	0.10
First-order Doppler shifts	0.00	0.50
Total, Sr <sup>+</sup>	522.3	1.3
Gravitational redshift	803.6	2.4
Total	1325.9	2.7

$\dagger \Delta\alpha_0 = -4.8314(20) \times 10^{-40} \text{Jm}^2/\text{V}^2$  [4].

Table 3: Maser noise coefficients for the one-sided fractional-frequency power-spectral-density (PSD) model,  $S_y(f) = h_2 f^2 + h_0 + h_{-1}/f + A/[1 + (f - f_0)^2/\delta f^2]$ .

White phase noise	$h_2$	$2.8 \times 10^{-24}$	$\text{Hz}^{-3}$
Flicker phase noise	$h_1$	$1.5 \times 10^{-26}$	$\text{Hz}^{-2}$
White frequency noise	$h_0$	$1.3 \times 10^{-27}$	$\text{Hz}^{-1}$
Flicker frequency noise	$h_{-1}$	$7.2 \times 10^{-33}$	1
Lorentzian peak	$A$	$6.5 \times 10^{-24}$	$\text{Hz}^{-1}$
	$f_0$	$5.0 \times 10^{-8}$	Hz
	$\delta f$	$5.5 \times 10^{-7}$	Hz

Table 4: Contributions to  $u_{\text{A/Lab}}$  and  $u_{\text{B/Lab}}$ .

Contribution	Uncertainty/ $10^{-15}$
Extrapolation (stochastic)	0.031
Extrapolation (drift)	0.0009
UTC(MIKE)-HM measurement and rounding	0.11
$u_{\text{A/Lab}}$ total	0.11
rf distribution/synthesis	0.020
$u_{\text{B/Lab}}$ total	0.020